CHAPTER 3

Surface preparation and characterization

The previous chapter presented a comprehensive literature review that revealed the significant effects of modified surface structures (Nano/Micro) on boiling heat transfer enhancement and critical heat flux. However, to achieve such performance requires good control over the coating layer thickness and surface texture. Therefore, one of the main objectives of this study is to fabricate a homogeneous and stable micro/nano textured coating that can improve the boiling heat transfer performance parameters. These parameters include nucleation site density, bubble growth, and bubble departure frequency [1-5], as well as surface characteristics such as roughness, and wettability [5-7].

3.1. Coating method and materials

The electrophoretic deposition (EPD) technique has been used to fabricate different types of composite coating layers of oxide nanoparticles on Cu substrates**.** In Chapter 2, it is already mentioned that EPD is a type of electrochemical method with several benefits over other techniques, such as high material efficiency, low energy consumption, easy to apply on complex shapes, a modest capital cost, and ease of scalability. The potential advantages and disadvantages of EPD and other conventional technique has presented in Table 3.1 briefly.

To study the effects of micro/nano textures on boiling heat transfer performance, various binary composites textured surfaces were prepared using TiO_2, SiO_2, and Al_2O_3 nanoparticles. Binary composites have many industrial applications such as composites of TiO_2-SiO_2 are used as self-cleaning and anti-reflectivity in solar industries, automobile and optical lenses [114]. Composite of Al_2O_3 and TiO_2 is used as corrosion resistive/ protective

layer on Cu, metals and other substrates, for electronic, mechanical, and optical applications [115]. The nanoparticles (powder form) were commercially purchased from AdNanotechnologies Pvt. Ltd. (Karnataka, India), and particle details are given in Table 3.2.

Fig. 3.1 illustrates a schematic representation of the electrophoretic deposition technique, in which two electrode cell assemblies are dipped into a nanofluid and connected to a DC power supply. In this process, charged particles dispersed in liquid move towards the oppositely charged conductive electrode (substrate that needs to be coated), when a DC electric field is applied across both electrodes.

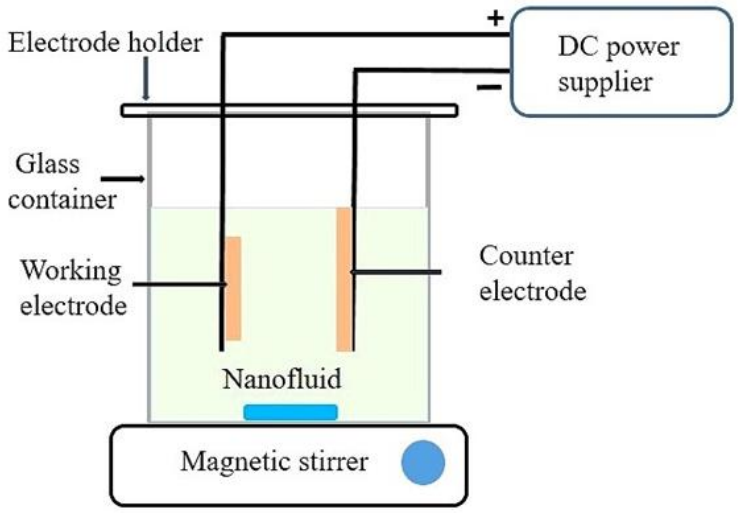

Fig. 3.1. Schematic illustration of electrophoretic deposition technique.

Because of the continuous accumulation of charge particles, reasonably compact, homogeneous, and thin film developed at the oppositely charged electrode (substrate).

To fabricate the composite micro/nanotextured surface, EPD was carried out in various steps: pre-treatment and polishing of base material, preparation of hybrid nanofluid, coatings of nanomaterial, removal of impurities, and surface drying. Fig. 3.2 shows the steps and their sequence, which was followed for the surface preparation.

Table 3.1. Potential advantages and disadvantages of EPD and other conventional technique

Techniques	**Pros**	**Cons**
Electrophoretic Deposition (EPD)	1. In this process charged particles suspended in a stable colloidal suspension and particle gets deposited on conductive substrate under an electric field. 2. Easy to apply on complex surface like cavities, convex, concave and spherical. 3. Easy control of coating composition and low energy consumption. 4. Initial setup and operating cost are modest. 5. No pre vacuum pressure and clean environment required to carried the process.	1. Non-conductive or poorly conductive materials are not suitable for EPD. 2. The particle size and distribution significantly impact the quality of the coating. 3. Achieving dense, void-free coatings can be challenging. 4. If the suspension settles or aggregates during deposition, it affects coating uniformity.
Chemical Vapor Deposition (CVD)	1. CVD is widely used to produce thin film coatings on semiconductor via various gaseous precursor. 2. Process occurs at low pressure hence coating is pure and good. 3. Process required low-vacuum gaseous environment than PVD	1. Challenging to produce multicomponent materials due to variations in nucleation, growth rate, and vapor pressure. 2. the process temperature is relatively high (Higher than the tempering temperature of HSS)

Table 3.1. Continue….

Physical Vapor Deposition (PVD)	1. PVD involves vaporizing a solid material and condensing it onto a substrate. 2. It can deposit alloys with controlled composition and can apply to any type of inorganic materials. 3. The obtained coating have great adhesion, resistance and durability. 4. PVD doesn't required any post treatment, therefore uses of chemical reagent is negligible, hence impact on environment is low. 5. No pre vacuum pressure and clean environment required to carried the process.	1. Some plasma damage, including implanted argon, may occur during PVD. 2. Coating speed is slow compared to EPD. 3. PVD has poor coating performance both on the back and side of the tool due to low air pressure. 4. Initial setup and operating cost is higher than EPD.
Atomic layer deposition (ALD)	1. ALD allows precise control over film thickness, which is critical for nanoscale devices. 2. It apply relatively good and uniform coatings on porous and high-aspect-ratio substrates. 3. Operates at low temperatures, hence damage is minimum to temperature sensitive materials.	1. ALD involves sequential, self-limiting reactions, which can be intricate to optimize. 2. Availability of suitable precursors limits the material choices. 3. Process is slow and required high vacuum condition, hence cost is very high.

Table 3.1. Continue….

Photolithography	1. In this process light is uses to produce precisely patterns of thin film over substrates like silicon wafers. 2. It can produce extremely small pattern up to a few tens of nanometre. 3. Process is comparatively fast and can create patterns over an entire silicon wafer at a relatively low cost. 4. It is commonly used to create pattern on various materials, including glass, silicon, and flexible substrates.	1. Photolithography faces limitations in making ultra-small structures and complex shape due to the category of light it uses. 2. It doesn't work well if substrate is not flat perfectly. 3. It involves several steps and requires skilled operators. 4. Requires clean environment where airborne particulate and chemical contaminants not exist. 5. Equipment coat is very high.

Table 3.2. Materials (nanoparticle) details

Sl. No.	**Nanoparticle materials**	**Bulk density (g/cm^3)**	**Shape**	**Average particle Size (nm)**
1	TiO_2	4.3	Nearly spherical	20-40
2	SiO_2	2.5	Spherical	20-50
3	Al_2O_3	2.25	Nearly spherical	20-50

3.1.1. Pre-treatment and surface polishing

In the first step, base copper surface (99 % pure) was cleaned with diluted sulphuric acid and DI water to remove the oxide layer from the surface. Then copper surfaces were polished with emery paper of grit sizes #1000, #1500, and #2000 [4], and cleaned with the help of ethanol and DI water in an ultrasonic bath (Model: GT-1730QTS) for 20 minutes. The photograph of ultrasonic bath is shown in Fig. 3.3.

3.1.2. Hybrid nanofluid preparation

In the second step, hybrid nanofluid was prepared with DI water using the two-step method [8]. Since, water has comparatively higher dielectric potential (78.5) compared to other base fluids such as ethanol (24.6), acetone (21.01), and ethylene glycol (24.6) at 20 °C. therefore it has been used as base fluid to achieve better dispersion and stability without any external agent. To prepare hybrid nanofluid of NP-1 (nanoparticle-1) and NP-2, each nanoparticle of equal weight (measured by a precise weight balance machine) has taken to form a 0.1 wt. % concentration of hybrid nanofluids. Since materials are in powder form so calculation of wt. % is more convenient and accurate than the volume concentration. The weight of nanoparticles was calculated using Eq. 3.1 to form a required wt. % concentration. Both nanoparticles were dispersed in 100 ml of DI water separately and sonicated for an hour with the help of a probe sonicator (LABMAN SCIENTIFIC INSTRUMENTS PVT. LTD., Model No: PRO-250, Fig. 3.4).

$$wt.\% = \left[\frac{wt_{np1}+wt_{np2}}{wt_{np1}+wt_{np2}+wt_{bf}}\right] \times 100 \quad (3.1)$$

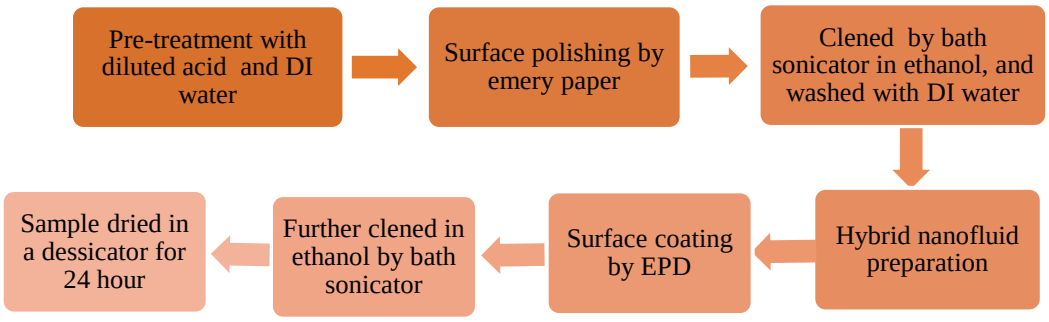

Fig. 3.2. Sequence of various activities which was followed in the surface coating by EPD method.

Fig. 3.3. Photograph of bath sonicator (Model: GT-1730QTS, Frequency: 33/40 kHz, Power: 100 W).

After sonication, NF-1 (nanofluid-1) and NF-2 are mixed in a single container and stirred for an hour with the help of a magnetic stirrer and then further sonicated for an hour with a probe sonicator; the resultant fluid is called a hybrid nanofluid of NP-1 and NP-2. The schematic representation of a two-step method is illustrated through a block diagram in Fig. 3.5.

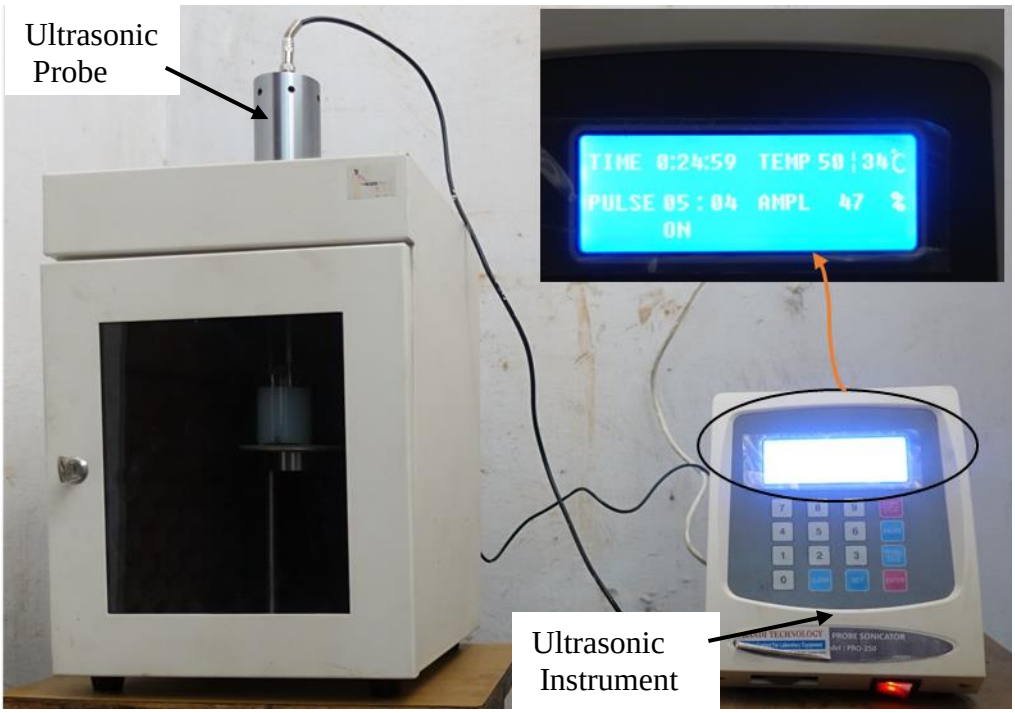

Fig. 3.4. Photograph of Probe sonicator (Frequency: 20 kHz, Power: 250 W)

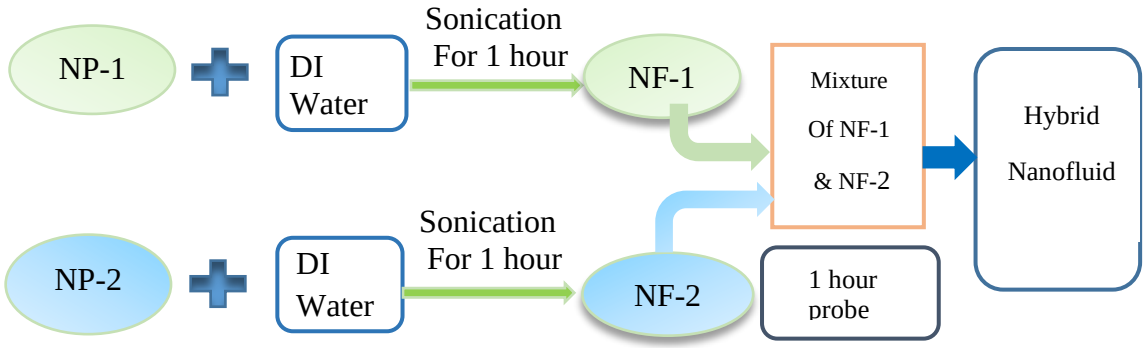

Fig. 3.5. Illustration of two-step method for hybrid nanofluid preparation.

Three different types of hybrid nanofluid were prepared and their dispersion stability was analysed using Malvern Zeta analyser. Figures 3.6 (a), 3.6(b), and 3.6(c) depicts the zeta potential distribution of TiO_2 – SiO_2, TiO_2-Al_2O_3, and SiO_2-Al_2O_3 hybrid nanofluids, respectively. The corresponding value of measured zeta potential are -37.2mV, -36.2mV, and -35.7mV which indicates good stability according to literature [9].

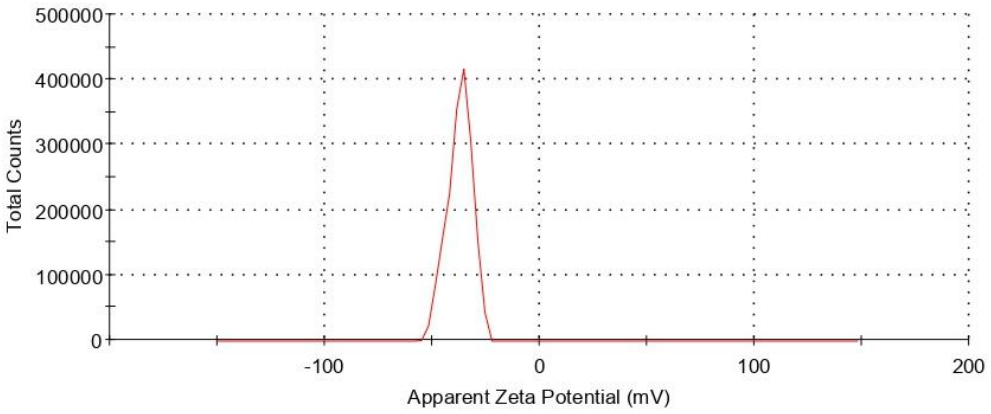

(a)

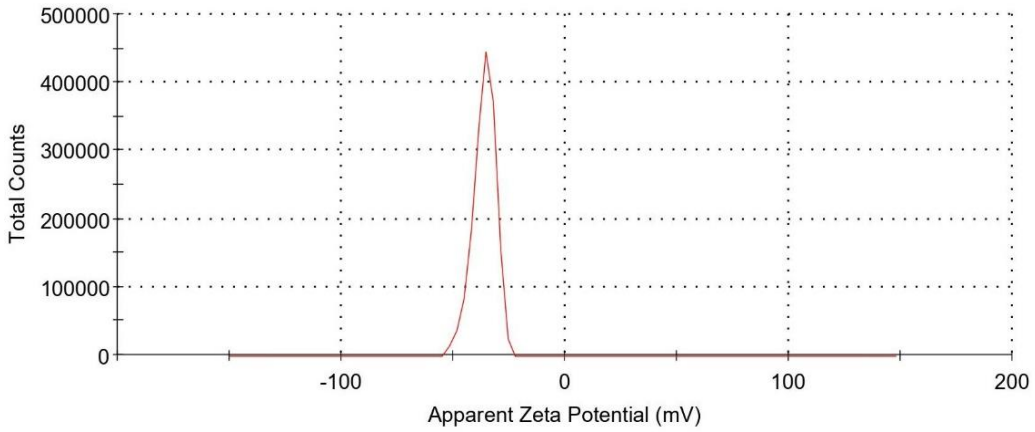

(b)

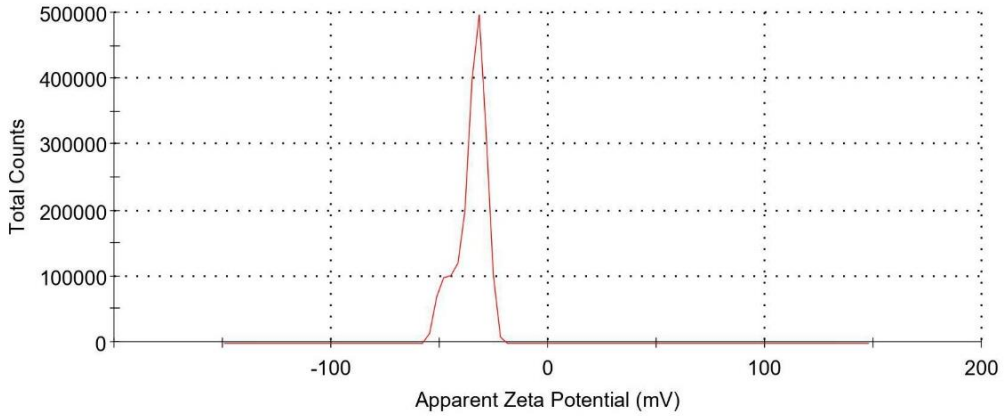

(c)

Fig. 3.6. Zeta potential distribution of (a) TiO_2 –SiO_2 (b) TiO_2 -Al_2O_3, and (c) SiO_2 -Al_2O_3 hybrid nanofluids (0.1 wt. %).

In the third step, the polished copper surface and electrode assembly were dipped in a hybrid nanofluid, and the coating was performed by passing a small DC current for a particular time [10]. In the present study, three different combinations of hybrid nanofluids have been used, and for each case, samples were fabricated by varying the coating time. The coating was performed over a circular disc (diameter 15.4 mm) of Cu substrates whose thickness is 0.6 mm and called the working electrode [11]. A counter electrode (also made of pure copper plate) is placed at a distance of 40 mm opposite to the working electrode, as shown in Fig. 3.1. In all three cases, coating occurs at the anode, therefore, the working electrode (sample that needs to be coated) is connected to the positive terminal (anode), while the counter electrode is connected to the negative terminal (cathode) of the DC power supply. After the coating, each sample was kept in an ultrasonic bath for 15 minutes in the medium of ethanol so that impurities on the coated surface were removed. Then all samples were allowed to dry for a minimum of 24 hours at room temperature in a desiccator. Once the sample is dried, it is ready for characterization tests and pool boiling performance investigation.

In every Electrophoretic Deposition (EPD) process, the hybrid nanofluid concentration was kept constant at 0.1 wt. %. The particle mixing ratio was also kept consistent at an equal percentage (1:1). Excluding the polished copper surface, a total of twelve samples were prepared. Table 3.3 presents the details of the hybrid nanofluid combination, concentration, particle mixing ratio, and variation in coating duration.

3.2. Surface characterization

Surface characterization such as morphology, coating layer thickness, wettability, and roughness of all the fabricated samples along with the polished Cu (bare) surface have been carried out, and their results are discussed in subsequent sections.

Table 3.3. Details of micro/nano composite coating parameters

Hybrid nanofluid used for coating	**TiO_2–SiO_2, and Water**	**TiO_2–Al_2O_3, and Water**	**SiO_2–Al_2O_3 with water**
Concentration of hybrid nanofluid (Wt. %)	0.1	0.1	0.1
Particle mixing ratio	Equal weight of both particle (1:1)	Equal weight of both particle (1:1)	Equal weight of both particle (1:1)
Current density (mA/cm^2)	15	20	20
Coating time (Minute)	5, 10, 15, and 20	2.5, 5, 10, and 15	5, 10, 15, and 20
Coating type	Anodic	Anodic	Anodic

3.2.1. Surface morphology

The boiling heat transfer significantly varied with the nature of the surface, like morphology and topography [13]. Surface morphology of all coated surface (CS) and bare surface (BS) are analysed using field emission scanning electron microscopy (FESEM) image.

3.2.1.1. TiO_2-SiO_2 coated surface

The coating was applied using the electrophoretic deposition technique, where TiO_2-SiO_2 hybrid nanofluid has been used. Four samples were prepared by varying the current duration to 5, 10, 15, and 20 minutes, which are referred to in the text as CS1-5, CS1-10, CS1-15, and CS1-20, respectively. For all four cases, the initial concentration of the hybrid nanofluid was kept at 0.1 wt. %.

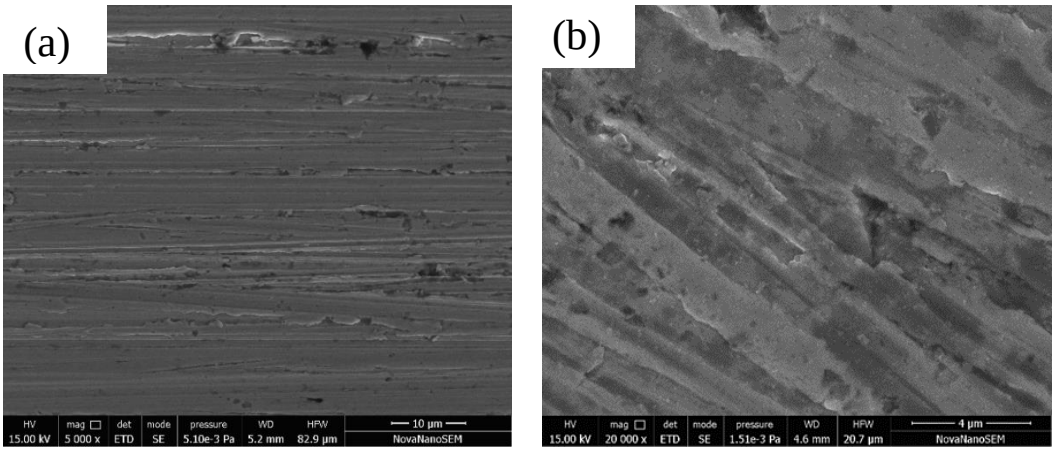

Fig. 3.7. FESEM image of polished (bare) Cu surface (a) 5000X (b) 20,000X

Fig. 3.7, and Fig. 3.8 depict FESEM images of a bare surface and TiO_2-SiO_2 coated surfaces, respectively. After comparing the image of bare and coated surfaces it is observed that the morphology of all coated surfaces is distinct from the bare one.

As the coating time varied, variations in surface morphology of coated samples (Fig. 3.8 (a), Fig. 3.8 (b), Fig. 3.8 (c), and Fig. 3.8 (d)) are also observed. Fig. 3.8 (a) represents the surface morphology of 5 minute coated sample (CS1-5), in which deposition of nanoparticles and structural changes are perceived. As the coating duration increased to 10 minutes (CS1-10), more nanoparticles were deposited, and developed large numbers of nanovoids on the surface, which can be seen in Fig. 3.8 (b). When the coating duration is increased to 15 minutes (CS1-15), the voids disappear and a large number of cone-shape cavities appear on the surface as shown in Fig. 3.8 (c).

Many of those cavities may activate during the boiling process with an increase in heat flux and act as nucleation sites. Also, there are many micro/nano hills like texturing visible on the surface. When coating time further increased to 20 minutes (CS1-20) cone shape cavities disappear and small cracks (Fig. 3.8 (d)) can be seen on the surface. This may be because of the longer duration of coating a dense, compact, and higher coating layer deposited on the surface.

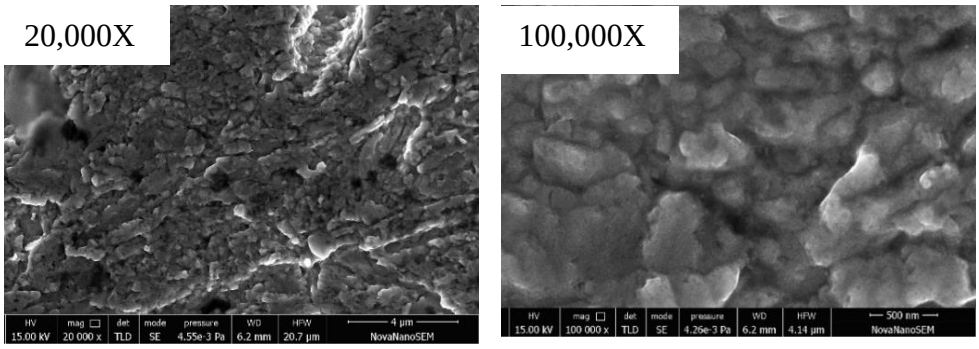

(a) 5 minute coating (CS1-5)

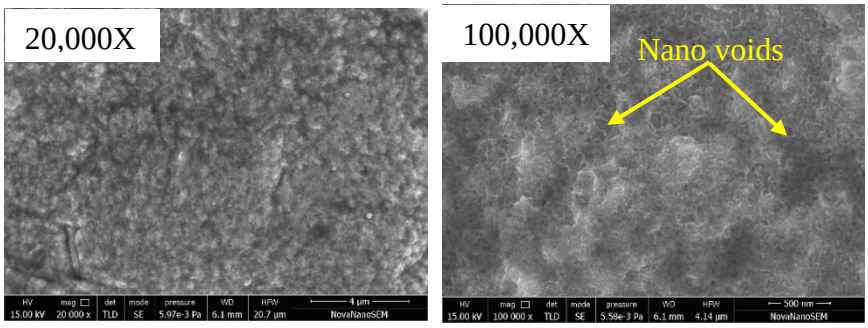

(b) 10 minute coating (CS1-10)

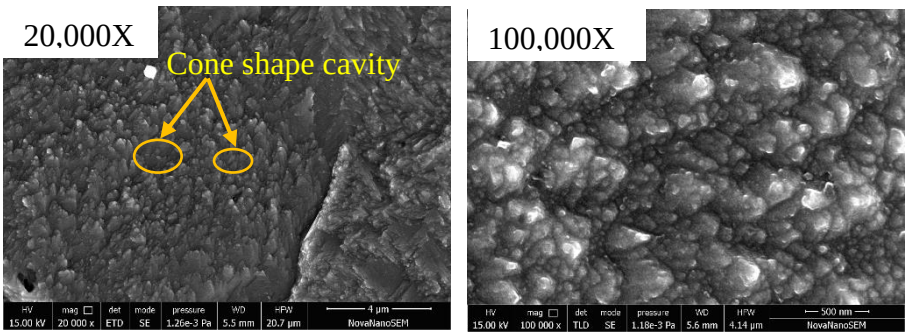

(c) 15 minute coating (CS1-15)

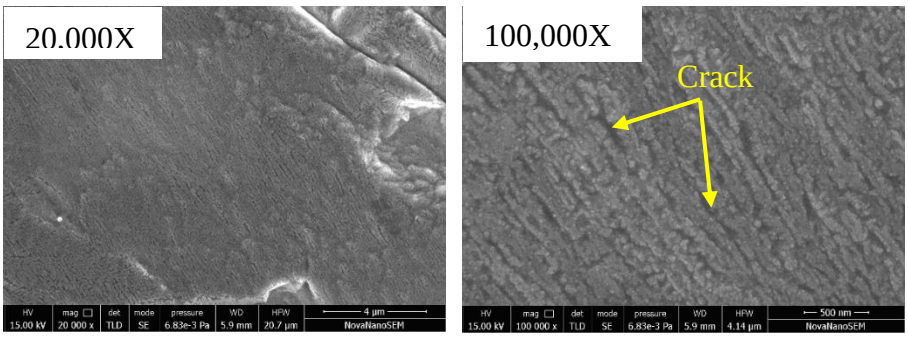

(d) 20 minute coating (CS1-20)

Fig. 3.8. Surface morphology (FESEM image) of TiO_2-SiO_2 coated surface at two different magnification.

3.2.1.2. TiO_2-Al_2O_3 coated surface

In this case, TiO_2-SiO_2 hybrid nanofluid has been used in the EPD process to fabricate the composite TiO_2-SiO_2 textured surface. Four different samples were prepared by varying the deposition times by 2.5, 5, 10, and 15 minutes at a current density 20 mA/cm^2, which are referred to as CS2-2.5, CS2-5, CS2-10, and CS2-15, respectively. Fig. 3.9 shows the surface morphology of newly fabricated composite textured surfaces. The surface morphology of all four coated surfaces looks different from the bare one. Also, realized that surface morphology varied with coating duration. When the coating time increased to 5 minutes, the patterns grew which is clearly visible in Fig. 3.9 (b), and identified many dimples type textured on the surface.

These dimples textured are in distinct shapes and sizes (micro and nanometer range). As the coating time increased to 10 minutes, the dimples textured disappeared from the surface (Fig. 3.9(c)) and various (width) very thin linings appeared on the surface, whose width and depth of in micro/nanometres. When coating time further increased to 15 minutes, due to continuous deposition of particles on the surface thin lining grew and converted into a nano-channel (width in nano range) type pattern (Fig. 3.9 (d)).

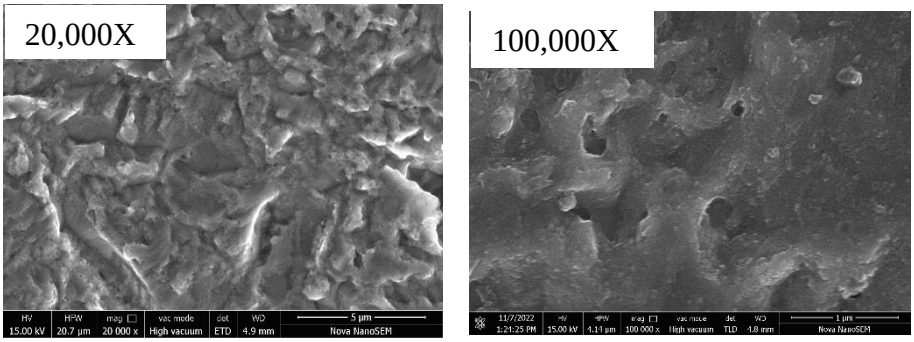

(a) 2.5 minute (CS2-2.5)

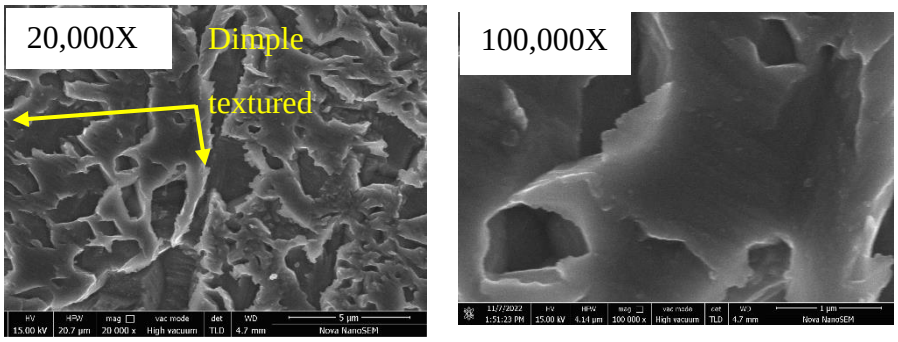

(b) 5 minute (CS2-5)

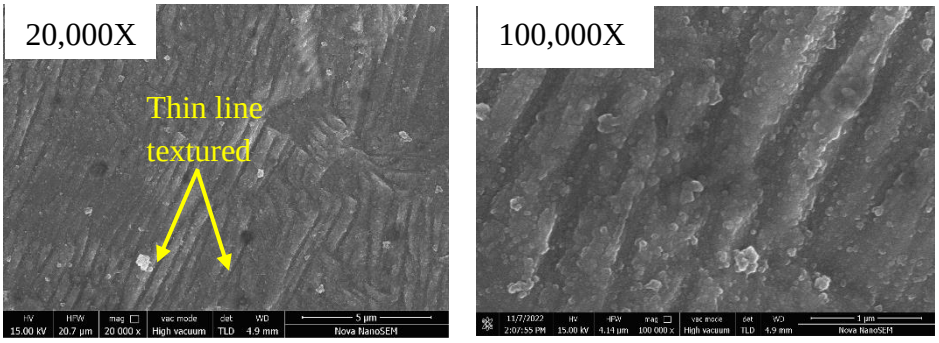

(c) 10 minute (CS2-10)

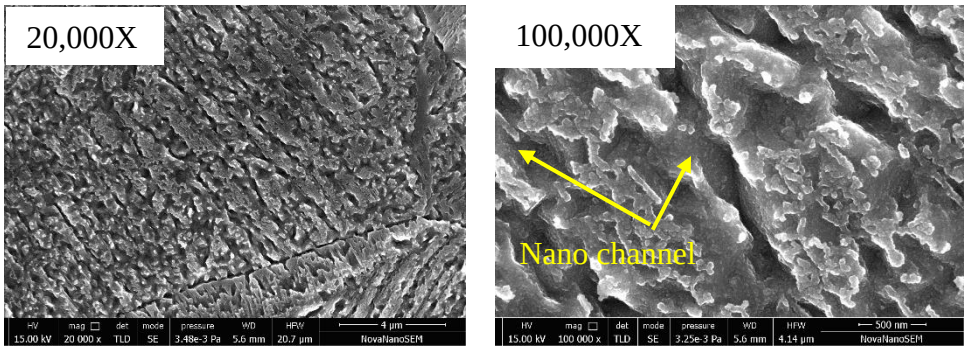

(d) 15 minute (CS2-15)

Fig. 3.9. Surface morphology (FESEM image) of TiO_2-Al_2O_3 coated surface (CS2) at 20k, and 100k magnification.

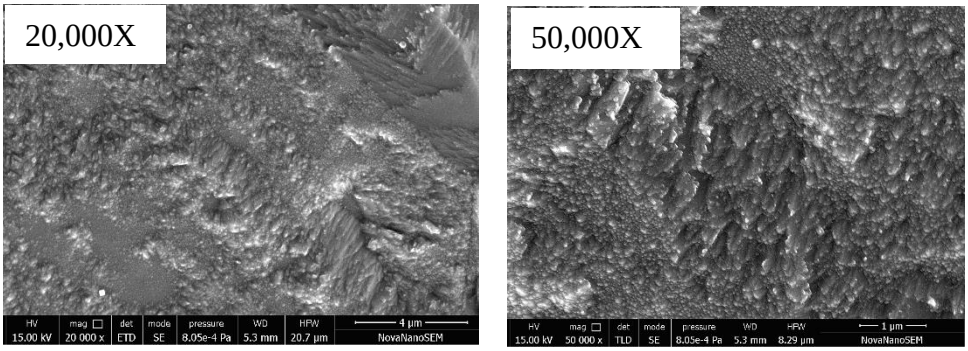

(a) 5 minute coating

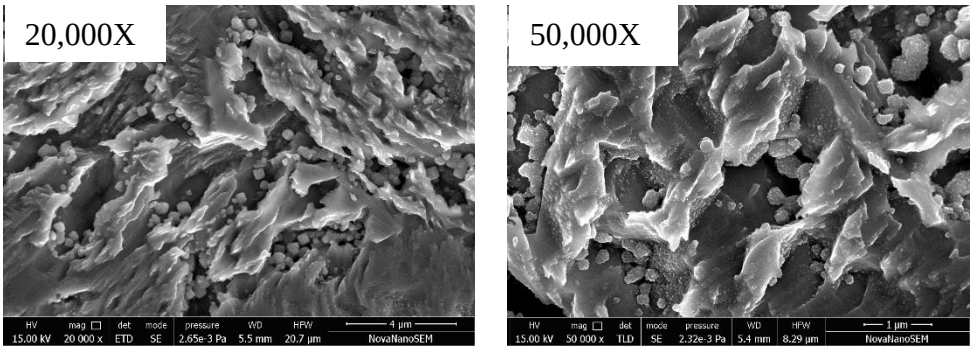

(b) 10 minute coating

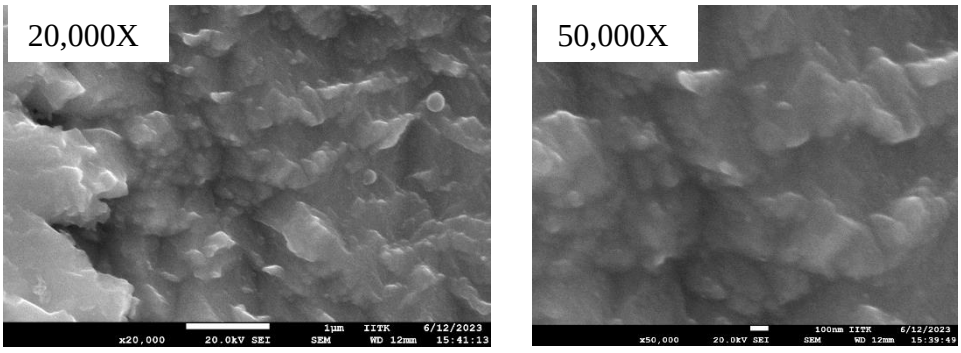

(c) 15 minute coating

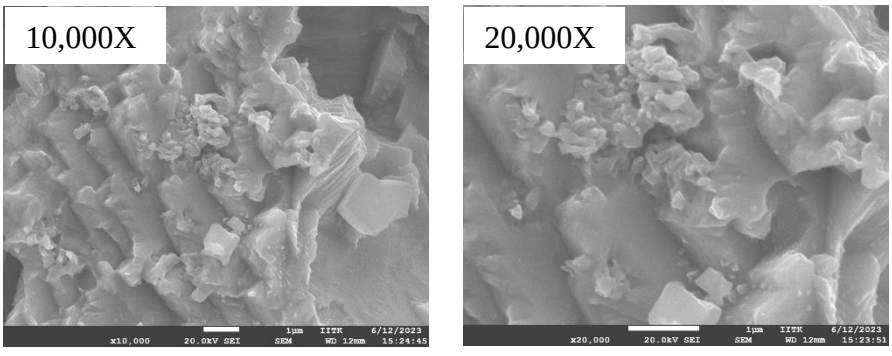

(d) 20 minute coating

Fig. 3.10. Surface morphology (FESEM image) of SiO_2-Al_2O_3 coated surface (CS3) at two different magnifications.

3.2.1.3. SiO_2-Al_2O_3 coated surface

This is the third combination where equal weight of SiO_2 and Al_2O_3 nanoparticle is used to prepare of hybrid nanofluid of 0.1 wt. % concentration. The composite textures were prepared by varying the coating duration 5, 10, 15, and 20 minutes at a current density of 20 mA/cm^2, which are referred to in the text as CS3-5, CS3-10, CS3-15, and CS3-20, respectively. The surface morphology of all newly fabricated surfaces is analysed by the FESEM image, and shown in Fig 3.10. The reader can notice that the structure (FESEM image) of CS1 (Fig. 3.8) and CS2 (Fig. 3.9) presented at higher magnification (max 100,000X), whereas CS3 (Fig. 3.10) presented at low magnification. The reason behind this is in former two cases structure was fine so it was not clearly identifiable at low magnification, while in later case structure was coarse and it was clearly identifiable at low magnification only. If we increase the magnification of coarse structure the image gets blur and only partial structure is visible, and pattern identification is challenging.

3.2.2. Energy Dispersive Spectroscopy (EDS) analysis

The elemental analysis of the textured surface is investigated through Energy Dispersive Spectroscopy (EDS) to confirm the presence of the coating element. The EDS spectrum of micro/nano textured surfaces of CS1-5, CS2-5, and CS3-5 are shown in Fig. 3.11, Fig. 3.12, and Fig. 3.13, respectively. In Fig. 3.11 presence of coated elements (Ti, Si, & O) is clearly visible with a small peak, where a higher peak represents the Cu element. Similarly in Fig. 12, and Fig. 13 also higher peak represents the Cu element, and the lower peak is marked with the respective coated elements present on the surface. In all EDS spectrum Cu element peak is very high due to the maximum weightage of Cu substrate with respect to coating materials.

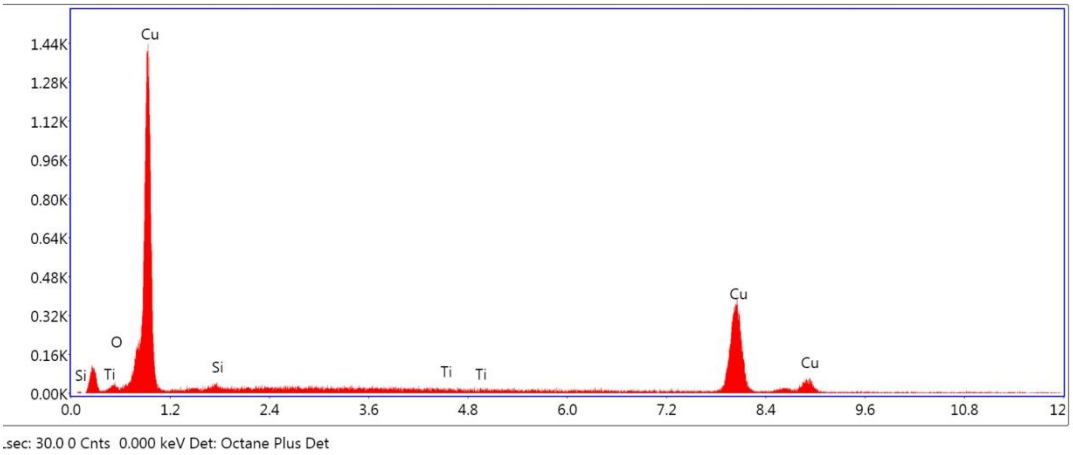

Fig.3.11. EDS spectrum of TiO_2-SiO_2 coated (CS1-5) surface.

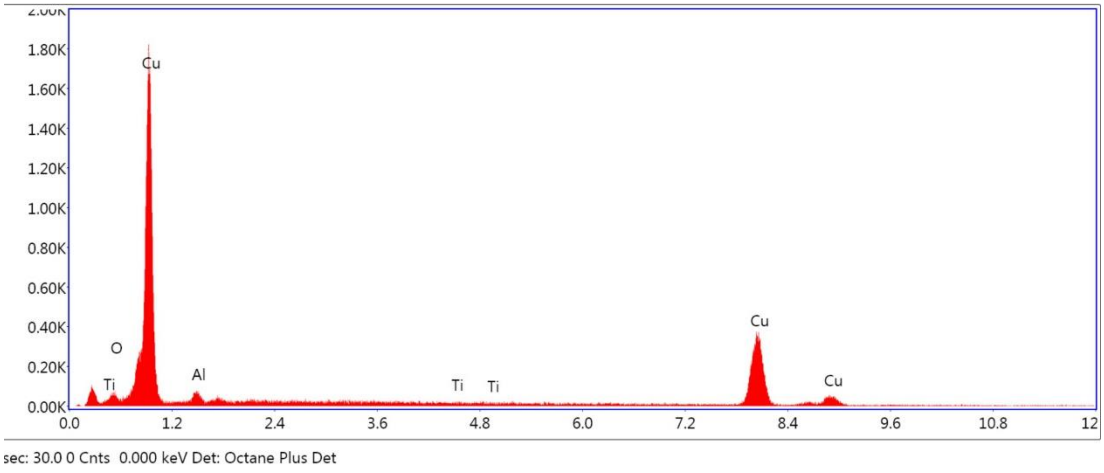

Fig.3.12. EDS spectrum of TiO_2-Al_2O_3 coated (CS2-5) surface

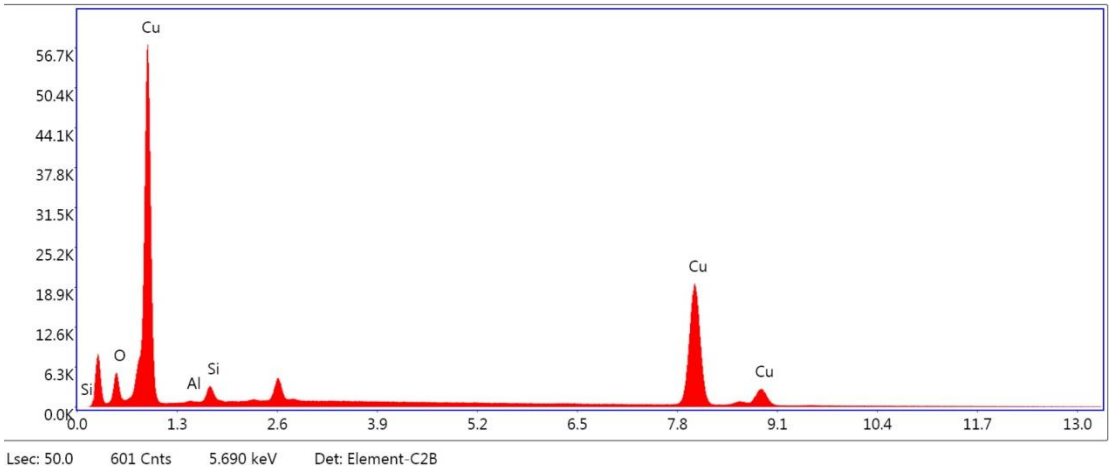

Fig.3.13. EDS spectrum of SiO_2-Al_2O_3 coated (CS3-5) surface.

3.2.3. Coating thickness

The cross-sections of the samples were observed using FESEM to measure the thickness of the coating layer. The FESEM images were analysed with ImageJ software and the results are presented in Fig. 3.14, Fig. 3.15, and Fig. 3.16. The vertical arrows in these figures show the locations where the coating layer thickness was measured and averaged. The average values are reported in respective figures. For all the cases coating thickness increased with an increase in coating time. However, coating thickness trends are distinct in all three (hybrid nanofluid) cases. A plot of coating layer thickness against coating duration has been drawn and shown in Fig. 3.17.

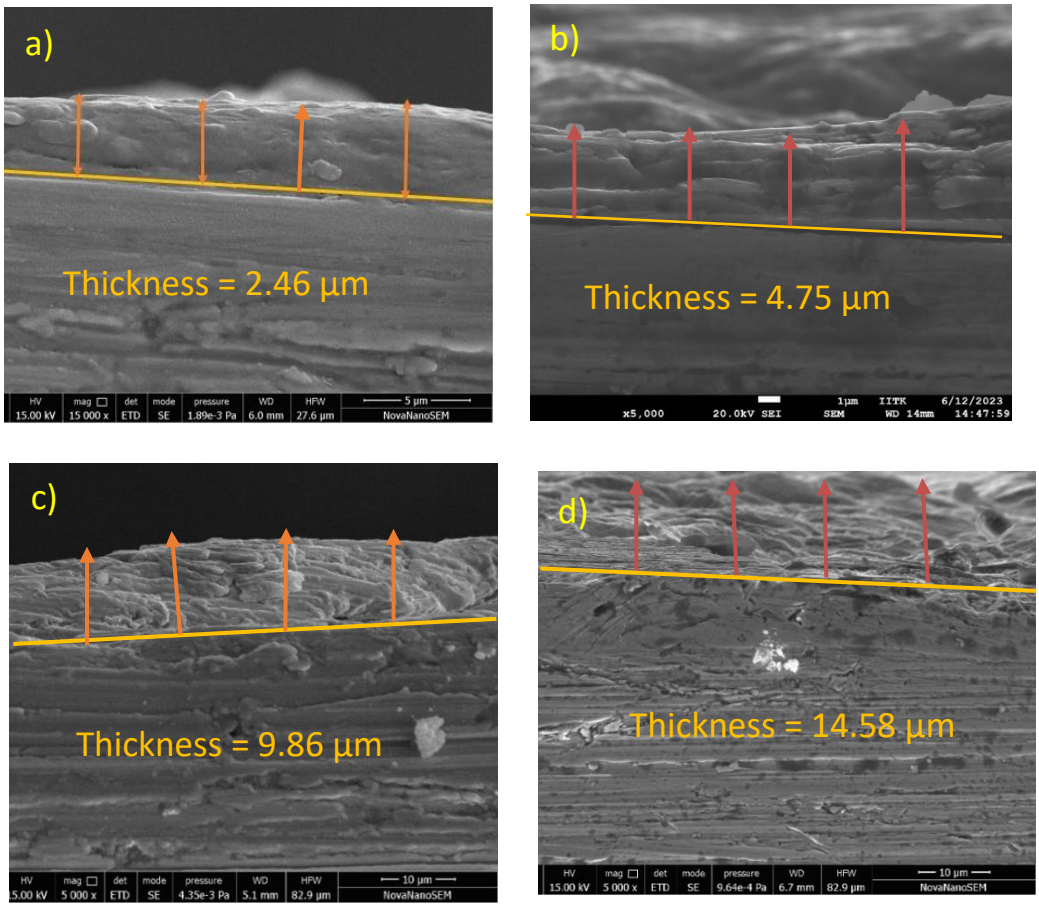

Fig. 3.14. Measurement of coating thickness (cross section image FESEM) of TiO_2-SiO_2 coated surface (a) CS1-5 (b) CS1-10 (c) CS1-15, and (d) CS1.

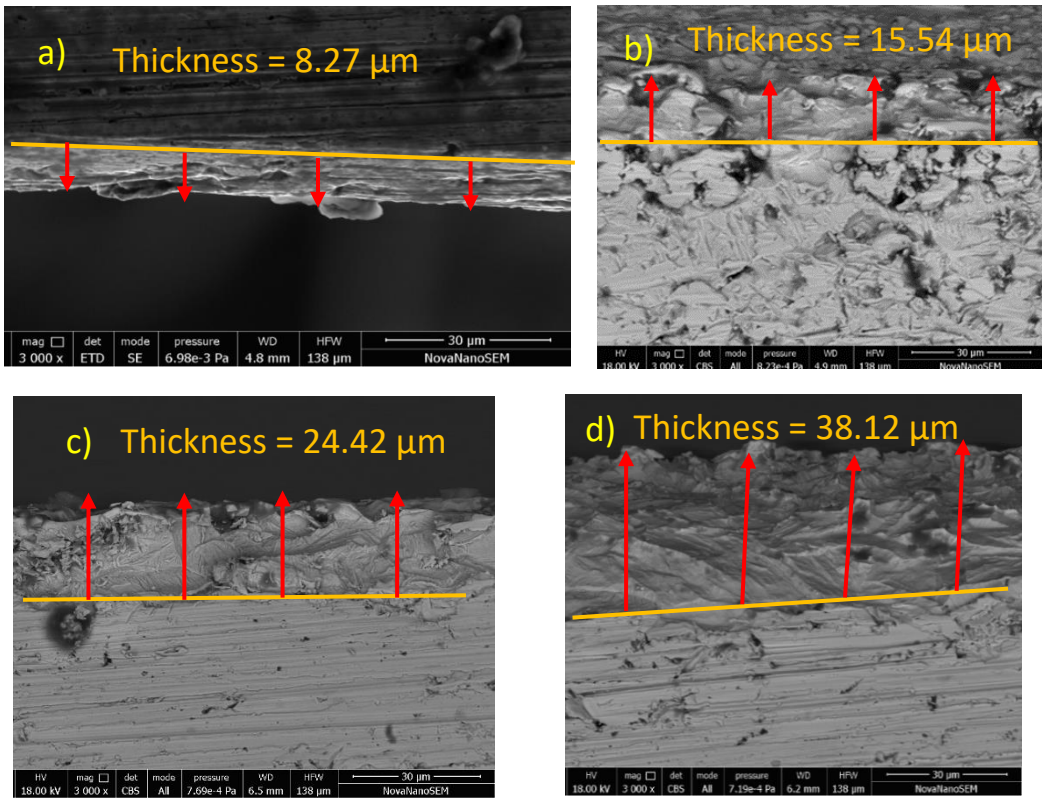

Fig. 3.15. Measurement of coating thickness (cross section image FESEM) of TiO_2-Al_2O_3 coated surface (a) CS2-2.5 (b) CS2-5 (c) CS2-10, and (d) CS2-15.

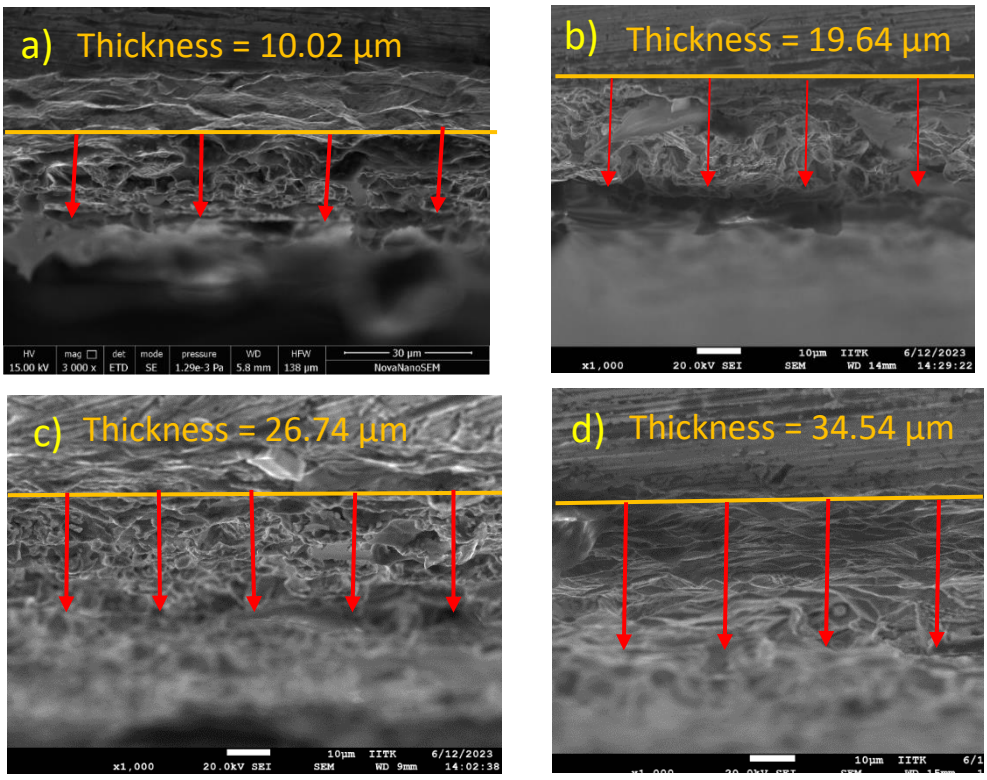

Fig. 3.16. Measurement of coating thickness (cross section image FESEM) of SiO_2-Al_2O_3 coated surface (a) CS3-5 (b) CS3-10 (c) CS3-15, and (d) CS3-20.

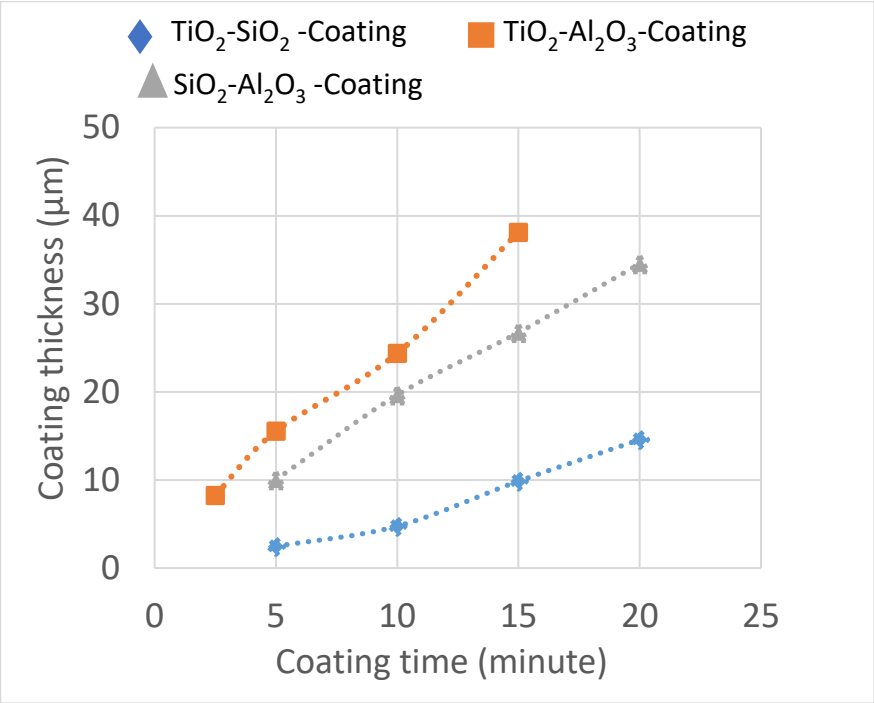

Fig. 3.17. Plot of coating thickness against the coating time

By looking at Fig. 3.17, it is clear that the variation of coating thickness in type-1 coating (TiO_2-SiO_2) and type-2 (TiO_2-Al_2O_3) coating is nearly linear fashion but have different slopes, while type-3 coatings (SiO_2-Al_2O_3) are nonlinear.

3.2.4. Surface roughness

The surface roughness of all the coated samples with bare Cu surfaces has been measured with the help of surface Profilometers. The roughness profile (waviness) of polished Cu and some coated samples (CS1–10, CS2–5, and CS3–10) are given in Figs. 3.18 and 3.19, respectively. The profilometer measures the roughness of a particular sampling length and gives the arithmetic mean value of roughness (Ra). Mathematically, the Ra value is expressed as Eq. (3.2), and it indicates the absolute average relative to the baseline.

$$R_a = \frac{\sum_{i=1}^{i=n} |y_i|}{n} \tag{3.2}$$

Where, y_i is difference in peak and valley height, and n is number of sampling in a particular length.

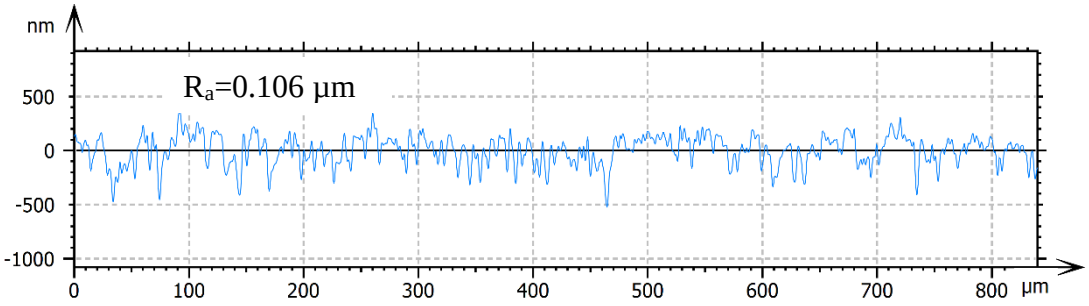

Fig. 3.18. Surface roughness profile of polished Cu (Bare) surface

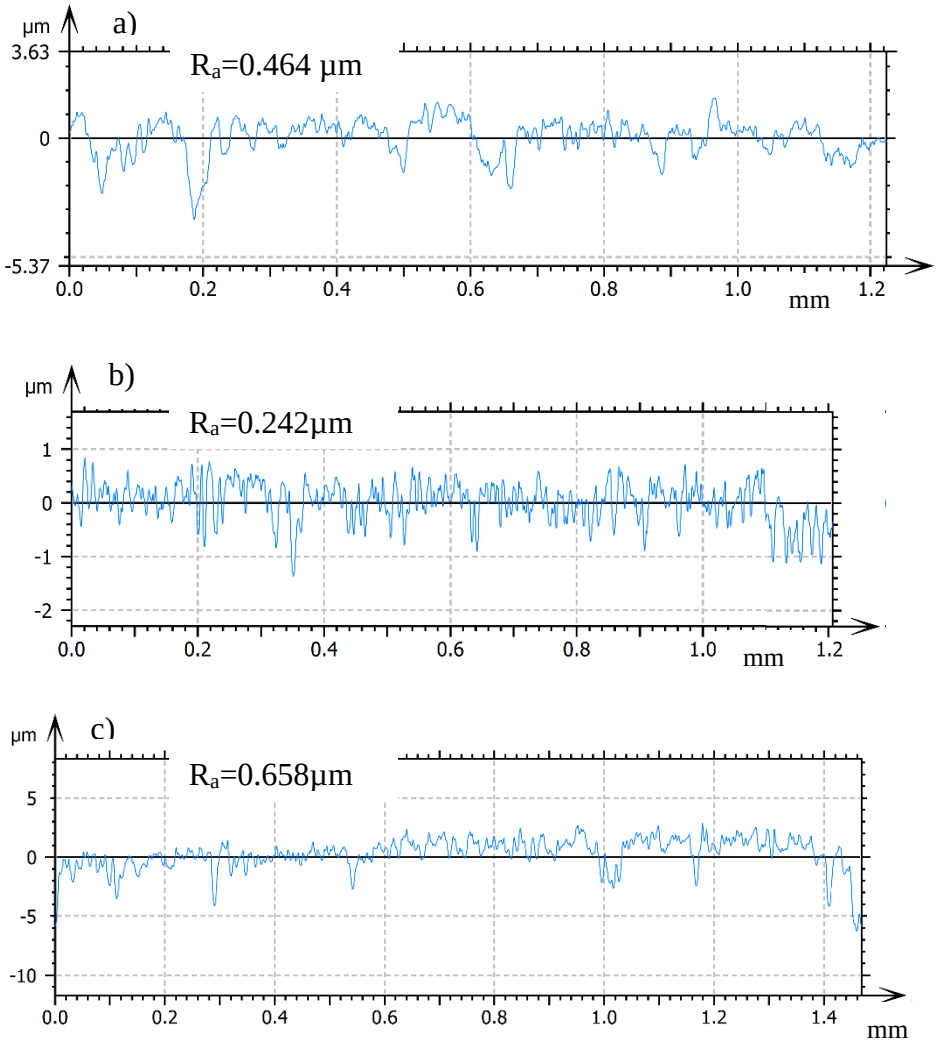

Fig. 3.19. Surface roughness profile of coated surface (a) CS1-10 (b) CS2-5, and (c) CS3-10.

The arithmetic mean value of surface roughness (Ra) of polished Cu (bare), and coated surfaces is presented in Table 3.4. By looking at Table 3.4, it is realised that all coated surfaces have a relatively higher roughness (Ra), than the bare surface. Also, with an increase in coating duration, the mean value of surface roughness (Ra) also increases. For the same coating duration SiO_2-Al_2O_3 coating has comparatively higher roughness than the other two, this may be because of course structure formation and higher average particle size of SiO_2 and Al_2O_3, nanomaterials than the TiO_2, which was uncommon in CS1 and CS2 composites.

Table 3.4. Arithmetic mean value of Surface roughness (R_a)

Surface roughness (µm)					
Polished Cu (Bare)	0.106				
Coating duration (minute)	2.5	5	10	15	20
TiO_2-SiO_2 coating	NA	0.194	0.271	0.464	0.653
TiO_2-Al_2O_3 coating	0.119	0.242	0.623	1.026	NA
SiO_2-Al_2O_3 coating	NA	0.430	0.658	0.880	1.40

3.2.5. Contact angle measurements/wettability analysis

Wettability characteristics of bare and coated surfaces were analysed with the help of contact angle measurements. The measurements of the static contact angle basically represent the wettability of a surface [12]. For hydrophilic ($\theta < 90°$) surfaces, a decrease in contact angle indicates wettability increases, while in the case of hydrophobic ($\theta > 90°$) surfaces, it decreases. In this study, contact angles were measured by a goniometer (Holmarc, model HO-IAD-CAM-01), which is equipped with a CCD camera and a syringe with a drop dispenser. A pictorial view of the goniometer facility is shown in Fig. 3.20. To measure the contact angle, a sessile

drop of volume 5 µl of DI water was generated with the help of drop dispenser and syringe on the sample. The image of sessile drop was captured through CCD camera, then image was processed and contact angle was measured with the help of ImageJ software as shown in Fig. 3.21. Similar procedure repeated for all samples and for each sample contact angle was measured at four different positions of the sample and average of all four measured value are presented in Table 3.5. Fig. 3.21 depict sessile drop image of the polished Cu (Bare), whereas Figs. 3.22, 3.23 and 3.24 depicts sample CS1, CS2 and CS3 respectively.

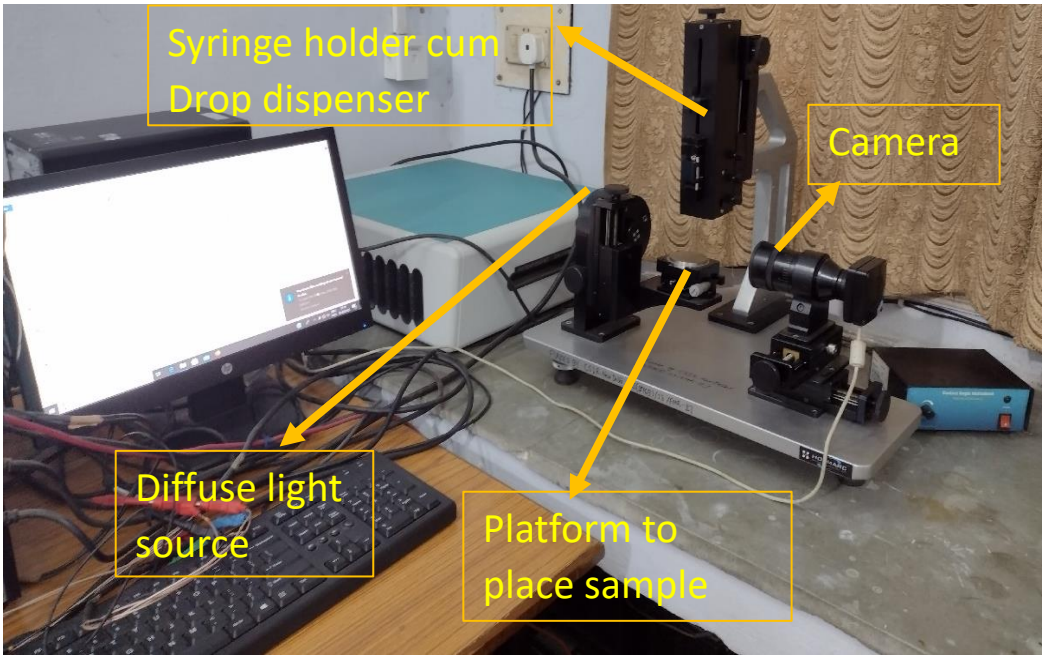

Fig. 3.20. Pictorial view of contact angle measurement facility (Goniometer, Holmarc, Model: HO-ED-M-01).

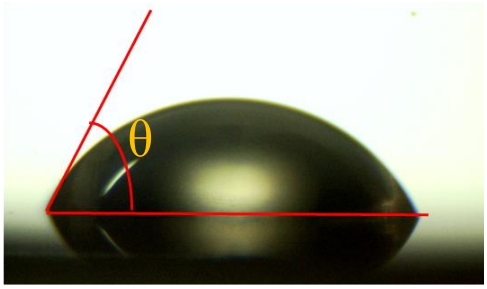

Fig. 3.21. Sessile drop image and contact angle measurement of a polished Cu (bare) surface.

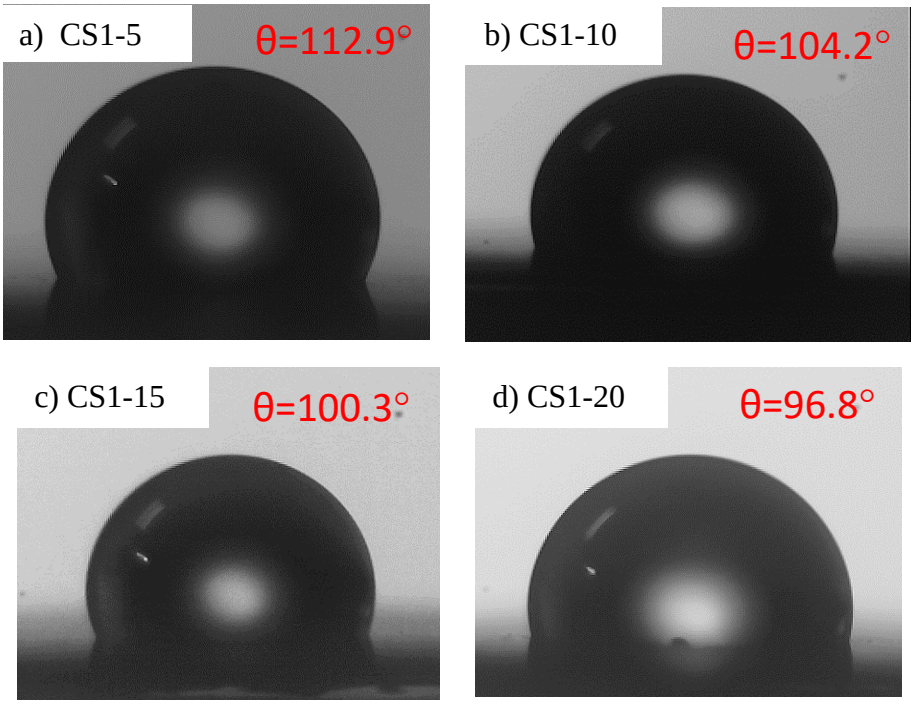

Fig. 3.22. Sessile drop image and contact angle measurement of TiO_2-SiO_2 coated surface.

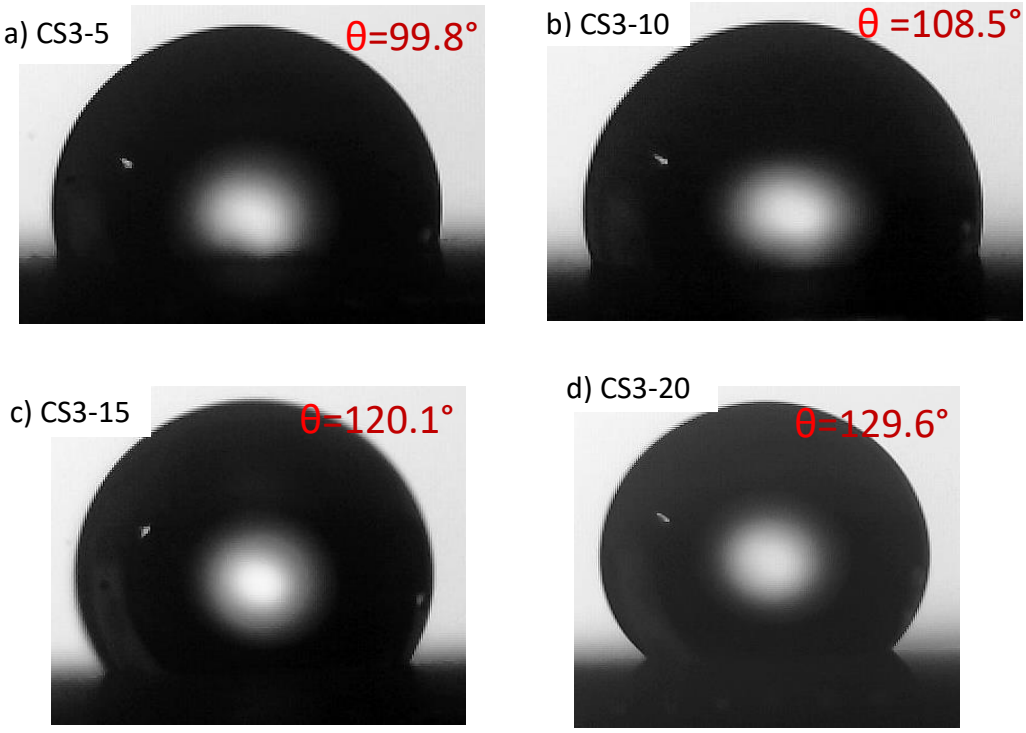

Fig. 3.23. Sessile drop image and contact angle measurement of TiO_2-Al_2O_3 coated surface.

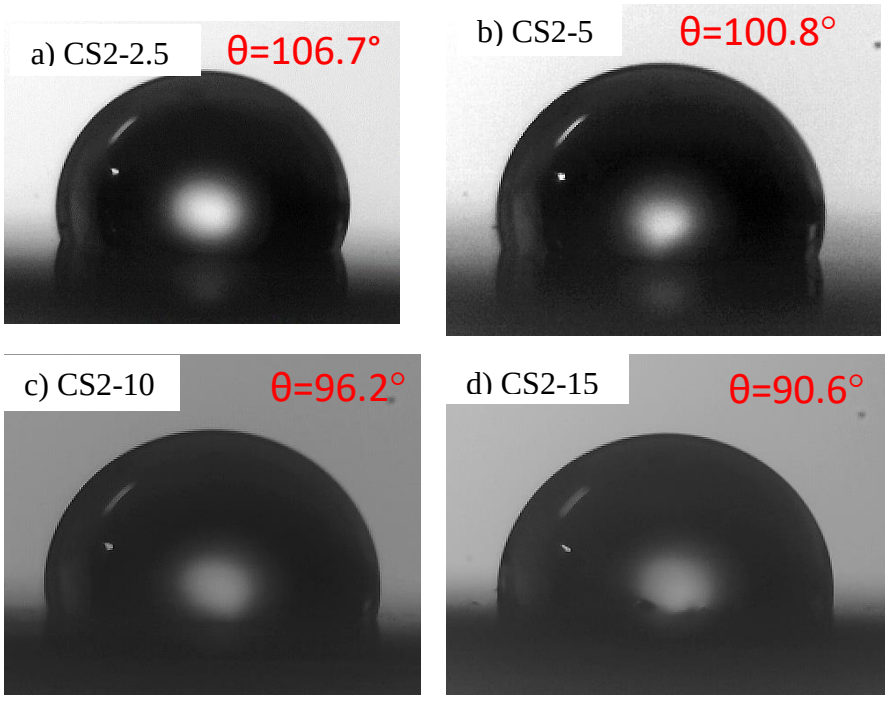

Fig. 3.24. Sessile drop image and contact angle measurement of SiO_2-Al_2O_3 coated surface.

Table 3.5. Results of contact angle measurements on bare and coated surfaces

Contact angle (°)					
Polished Cu (Bare)	65.7° (*)				
Coating duration (minute)	2.5	5	10	15	20
TiO_2-SiO_2 coating	NA	112.9° (#)	104.2°(#)	100.3°(#)	96.8° (#)
TiO_2-Al_2O_3 coating	106.7°(#)	100° (#)	96.2° (#)	90.6° (#)	NA
SiO_2-Al_2O_3 coating	NA	99.8° (#)	108.5° (#)	120.1° (#)	129.6° (#)

*Hydrophilic in nature, #Hydrophobic in nature

Results of contact angle measurement indicate that the bare surface is hydrophilic in nature, whereas all coated surfaces are hydrophobic in nature which is different from most reported studies. In most of the boiling heat transfer literature it has reported that the oxides particles form hydrophilic coating on copper substrate [88-89]. But some literature like Yulin et al. [116] and Jianying et al. [117] has prepared TiO_2 thin film as self-cleaning hydrophobic surface with the help of external agents. Yulin et al. [116] used ethanol and stearic acid to modify the TiO_2 as hydrophobic, whereas Jianying et al. [117], used polymer matrix (low surface energy material) and developed a multifunctional TiO_2 hydrophobic thin film. In another study Rosales et al. [114] has synthetized hydrophobic composites of TiO_2-SiO_2 and reviewed its applications.

As discussed earlier (section 3.2.1) that the composites structures forms micro/nano voids, and dimples on the composite surfaces. According to Rosales et al. [114], the combination of micro and nano structures creates rugosity in the surface which is a prime cause of the hydrophobic behaviour. Addition to this ethanol has used to clean the surface just after EPD which also be another reason behind hydrophobicity of all surfaces. To verify the individual coating wettability three surfaces were prepared with similar procedure in TiO_2, SiO_2, and Al_2O_3 nanofluids separately, and contact angle was measured. The contact angle results indicated that the surfaces prepared in individual nanoparticles are also have hydrophobic nature. Therefore, surface prepared in mixture of these oxides' particles concurred with their individual nature.

In comparison to the bare surface, the wettability of the textured surface decreases. For the case of TiO_2-SiO_2 (CS1) and TiO_2-Al_2O_3 coating (CS2) the contact angle decreases, which means wettability increases as the coating duration increases, whereas in the case of SiO_2-Al_2O_3 coating (CS3), contact angle increased, therefore wettability decreases with increase in coating duration. In the latter case contact angle increases as coating duration increases, this may be because of micro/nano structures getting coarser with coating duration

(Fig. 3.10). According to Giacomello et al. [118] surface texturing is another way to decrease the surface energy**.** Hence the fractional variation in micro/ nano texture of SiO_2-Al_2O_3composite may be higher as coating duration increases, causes contact angle (Hydrophobicity) increases.

3.3. Summary

The surface preparation and characterization are presented in this chapter. Electrophoretic deposition technique was used to fabricate different composite textures. Three different particle combinations (TiO_2-SiO_2, TiO_2-Al_2O_3, and SiO_2-Al_2O_3) have been used to prepare hybrid nanofluids by the two-step method. Different composite textures have prepared by passing a small DC current for four distinct durations. The developed textured surface is characterised and compared with a polished Cu (bare) surface. Characterization results showed that the surface morphology of coated (textured) surfaces is different from the bare surface. With an increase in coating duration, surface texture also changes. It is realised that up to a certain duration, structures grow, develop, and appear clearly on the surface, beyond that structures start disappearing from the surface. To confirm the deposited elements, EDS has been done where the presence of coated elements has been confirmed. Coating thickness was measured by analysing the cross-section of the sample with a FESEM image. Coating thickness is observed to increase with coating duration; however, the rate of increase depends on the nanoparticle combination. Surface roughness was measured by a Profilometer, and it was found that surface roughness also increased with increases in coating duration.

****